AIP | Journal of Applied Physics

Exchange bias induced by the fully strained La2/3Ca1/3MnO3 dead layers

Q. Y. Xie, X. S. Wu, J. Gao, and Q. J. Jia

Citation: Journal of Applied Physics **115**, 17D701 (2014); doi: 10.1063/1.4857935
View online: http://dx.doi.org/10.1063/1.4857935
View Table of Contents: http://scitation.aip.org/content/aip/journal/jap/115/17?ver=pdfcov
Published by the AIP Publishing

Articles you may be interested in

Unexpected ferromagnetic ordering enhancement with crystallite size growth observed in La0.5Ca0.5MnO3 nanoparticles
J. Appl. Phys. **116**, 113901 (2014); 10.1063/1.4895707

Cooling-field dependence of exchange bias effect in La0.45Sr0.55MnO3 nanoparticles
J. Appl. Phys. **116**, 043913 (2014); 10.1063/1.4890723

Coexistence of considerable inter-particle interactions and spin-glass behavior in La0.7Ca0.3MnO3 nanoparticles
J. Appl. Phys. **115**, 17B504 (2014); 10.1063/1.4862522

Impact of reduced dimensionality on the magnetic and magnetocaloric response of La0.7Ca0.3MnO3
Appl. Phys. Lett. **102**, 062414 (2013); 10.1063/1.4792239

Magnetic properties of Sm0.1Ca0.9MnO3 nanoparticles
J. Appl. Phys. **112**, 063921 (2012); 10.1063/1.4754310

HIDEN ANALYTICAL
Instruments for Advanced Science

Contact Hiden Analytical for further details:
W www.HidenAnalytical.com
E info@hiden.co.uk
CLICK TO VIEW our product catalogue

Gas Analysis
- dynamic measurement of reaction gas streams
- catalysis and thermal analysis
- molecular beam studies
- dissolved species probes
- fermentation, environmental and ecological studies

Surface Science
- UHV TPD
- SIMS
- end point detection in ion beam etch
- elemental imaging - surface mapping

Plasma Diagnostics
- plasma source characterization etch and deposition process reaction
- kinetic studies
- analysis of neutral and radical species

Vacuum Analysis
- partial pressure measurement and control of process gases
- reactive sputter process control
- vacuum diagnostics
- vacuum coating process monitoring

[This article is copyrighted as indicated in the article. Reuse of AIP content is subject to the terms at: http://scitation.aip.org/termsconditions. Downloaded to] IP: 147.8.204.164 On: Fri, 19 Sep 2014 07:33:12

Exchange bias induced by the fully strained $La_{2/3}Ca_{1/3}MnO_3$ dead layers

Q. Y. Xie,[1,2] X. S. Wu,[1,a)] J. Gao,[3] and Q. J. Jia[4]
[1]*National Lab of Solid State Microstructures, Department of Physics, Nanjing University, Nanijng 210093, People's Republic of China*
[2]*College of Electronic Science and Engineering, Nanjing University of Posts & Telecommunications, Nanjing 210046, People's Republic of China*
[3]*Department of Physics, The University of Hong Kong, Pokfulam Road, Hong Kong*
[4]*Institute of High Energy Physics, Chinese Academy of Sciences, Beijing 100039, China*

(Presented 7 November 2013; received 9 September 2013; accepted 11 October 2013; published online 7 January 2014)

A pure compressively strained $La_{2/3}Ca_{1/3}MnO_3$ (LCMO) dead layer grown on (001)-oriented $LaAlO_3$ substrate can show all the rich phenomenon of large bias field shift, coercive field enhancement, and high blocking temperature. The obtained exchange bias field (~350 Oe) and the enhanced coercivity of about 1160 Oe at 5 K under 500 Oe cooling field are superior to that have been reported in LCMO-based ferromagnetic/antiferromagnetic superlattices or nanoscale systems. Our results clearly demonstrate that the inhomogeneous magnetic dead layer of LCMO can induce a strong exchange bias effect, which may be exploited as a very simple structure for spin-valve device application. © *2014 AIP Publishing LLC*. [http://dx.doi.org/10.1063/1.4857935]

I. INTRODUCTION

Perovskite manganite oxide $La_{2/3}Ca_{1/3}MnO_3$ (LCMO)[1,2] exhibits a notably rich research interests due to its half-metallic character, colossal magnetoresistance (CMR) response, and a possibility to employ it in spin-electronic device applications. Earlier investigation[3] has established that the ultrathin LCMO film may act as "dead-layer" compared with its bulk, showing insulating behavior and depressed magnetization. An extensive body of work provides some excellent explanations on the presence of this dead layer, which including electronic phase separation of charge-ordered insulating and ferromagnetic metallic regions,[4] structure change from bulk *Pnma* to body-centered *Imma* space group,[5] and orbital reconstruction.[6] However, the insulating behavior and depressed magnetization generally made the study to the dead layer is still rather limited. So far, the spin state of dead layer among many oxide systems still remains controversy. Motivated by the desire to uncover the magnetic state of LCMO dead layer, we have carried out a comprehensive experimental study which can surely extend our understanding of the ultrathin film.

A. EXPERIMENTAL DETAILS

Ultrathin films of $La_{2/3}Ca_{1/3}MnO_3$ have been synthesized and characterized. In this paper, LCMO layers were grown on (001)-oriented $LaAlO_3$ (LAO) substrate by modified off-axis magnetron sputtering method with details described elsewhere.[2] Four ultrathin films with the thickness of 3 nm (L3), 6 nm (L6), 12 nm (L12), and 24 nm (L24) are discussed. One 42 nm thick film (L42) is also prepared for comparison. X-ray diffraction (XRD) and grazing incidence X-ray diffraction (GIXRD) measurements were carried out at a Rigaku Dmax-rB diffractometer with CuKα radiation in addition to use the Beijing Synchrotron Radiation Facility. The magnetic measurements were measured with the superconducting quantum interference device (SQUID).

II. RESULTS AND DISCUSSIONS

Figures 1(a) and 1(b) show the experimental and simulated X-ray reflectivity (XRR) curves for typical L3 and L42, respectively. The fit suggests very smooth surface morphology with the roughness below 0.6 nm, indicating a coherence layer-by-layer growth mode. Fig. 1(c) exemplifies the XRD pattern recorded around the (002) peak of LAO substrate for all the LCMO films. With the increase of film thickness, the intensity of LCMO (002) peak increases and peak becomes narrower but the peak position does not change up to 24 nm. The L42, on the other hand, shows strain relaxation, with a clear movements of LCMO (002) peak to larger angles.

The corresponding out-of-plane lattice parameter is calculated and shown in Fig. 2(a), indicating four ultrathin films grow compressively strained. Fig. 2(b) shows the GIXRD pattern of typical L12 film and the corresponding in-plane lattice parameter ($a_{\parallel}$) as a function of penetration depth is displayed in the inset of Fig. 2(b). One can see the in-plane lattice parameter is roughly independent on the penetration depth, which is a strong evidence of fully strained state. For fully strained L12, the effective unit cell volume is $V_{eff} = a_{\parallel}^2 a_{\perp} = 56.7$ Å^3, smaller than that of the partially relaxed L42 ($V_{eff} = 57.3$ Å^3). The contracted unit cell volume, as compared to the bulk stoichiometric samples of LCMO (57.42 Å^3), has been proposed to be a relative higher concentration of tetravalent manganese ions in the manganite layer than that in the target (33%).[7] Therefore, continuing the analogy with the Ref. 7, for our ultrathin films considered one would expect the stain-enhanced phase separation.

To test this hypothesis, we carried out magnetic measurements, as shown in the Fig. 3(a). With decreasing film thickness, the magnetization decreases strongly. Moreover,

a)Author to whom correspondence should be addressed. Electronic mail: xswu@nju.edu.cn. Fax: +86 25 83594402.

 © 2014 AIP Publishing LLC

[This article is copyrighted as indicated in the article. Reuse of AIP content is subject to the terms at: http://scitation.aip.org/termsconditions. Downloaded to] IP: 147.8.204.164 On: Fri, 19 Sep 2014 07:33:12

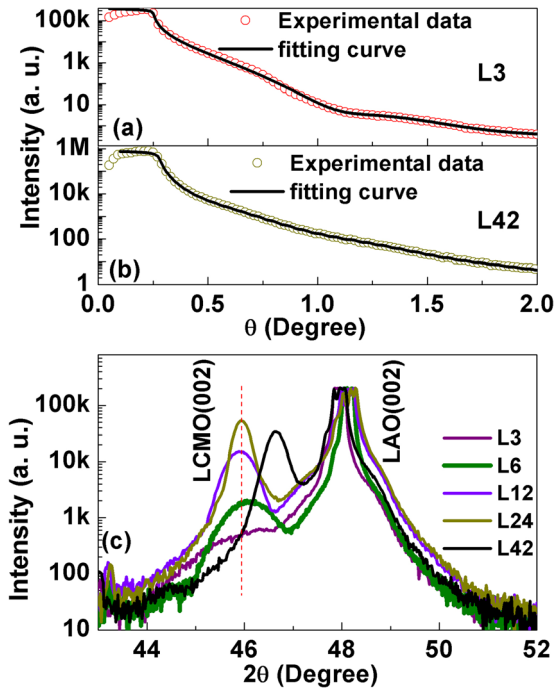

FIG. 1. X-ray reflectivity curves for L3 (a) and for L42 (b). (c) Room temperature X-ray diffraction pattern of LCMO thin film with different thicknesses.

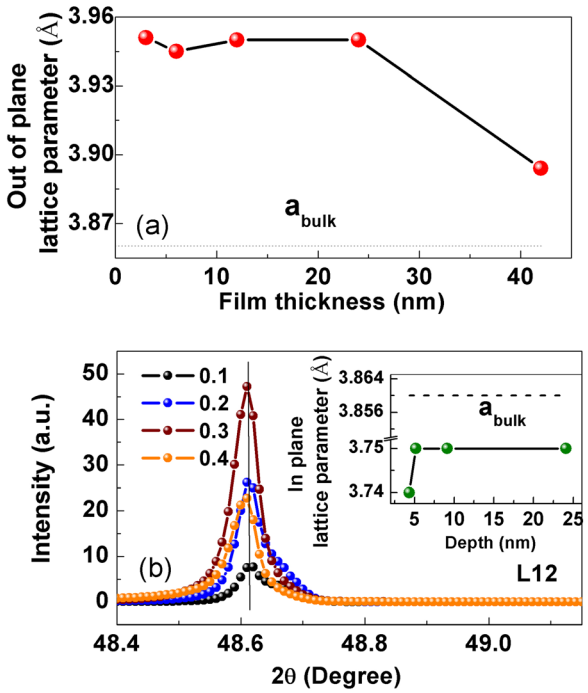

FIG. 2. (a) The thickness dependence of out-of-plane lattice parameter for studied films. (b) Grazing incidence X-ray diffraction pattern of L12 at different incidence angles. The inset shows the in-plane lattice parameter of L12 as a function of penetration depth.

the zero field cooling (ZFC) M-T curves of LCMO ultrathin films are identified with a pronounced peak (freezing temperature T_f, as indicated by the arrow in Fig. 3(a)), which is accompanied by a large bifurcation between ZFC and field cooling (FC) process. This character is often considered as the signature of spin/cluster glass state due to the magnetic frustration between the ferromagnetic (FM) double exchange and antiferromagnetic (AFM) superexchange interactions.[3] The LCMO dead layer has been shown to induce chemical or electronic phase transition easily. For example, a cationic segregation progress of La atoms towards the surface of film was reported in LCMO/LAO heterostructure by transmission electron microscopy,[8] which explained the magnetic properties. Nuclear-magnetic-resonance[9] revealed that the coexistence of FM clusters and antiferromagnetic charge-ordered clusters. Moreover, as proposed theoretically by Fang *et al.*,[10] the increase of tetragonal distortion c/a is a measure of the strength of FM metallic phase and C-type AF orbital-ordering phase. Compared with ideal FM phase environment (c/a = 1), the c/a ratio of about 1.04 for our LCMO dead layer indicates the possible coexistence of FM and AFM clusters should be considered.

Further, for L3–L24 films, a clear shift of the centre of magnetic loop towards the negative field direction is observed after field cooling from room temperature under the magnetic field of 500 Oe. While for the ZFC process, the hysteresis is normal. The behavior put towards the exchange

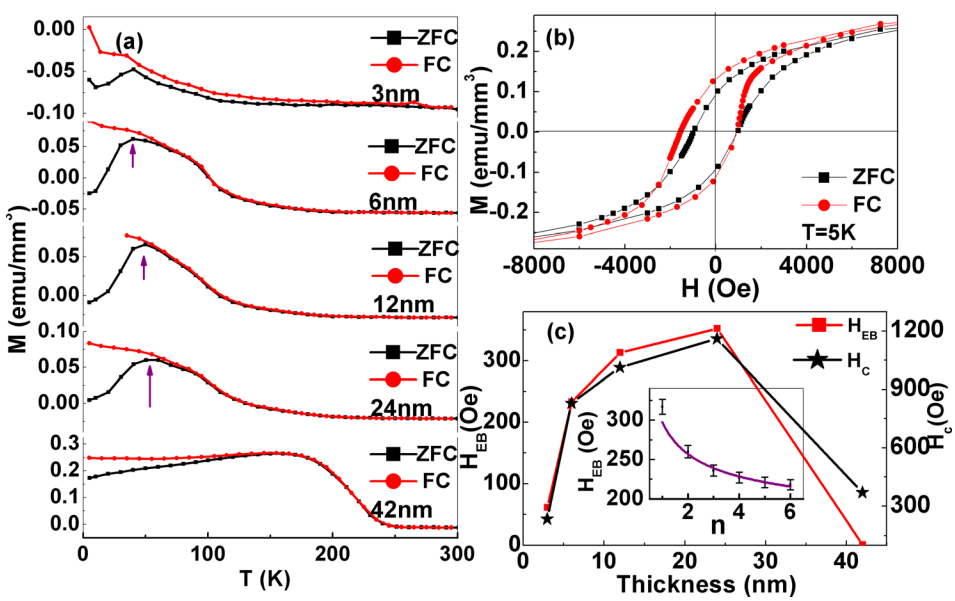

FIG. 3. (a) Temperature dependence of magnetizations with ZFC and FC processes for L3, L6, L12, L24, and L42, respectively. (b) Hysteresis loops of L24 at 5 K measured after zero-field cooling and field cooling in 500 Oe field. (c) Thickness dependence of H_{EB} and Hc at 5 K. The inset is the number of filed cycles n dependence of H_{EB} for L12. The cooling field is set to 500 Oe. Solid line shows the best fit to the data for n > 1.

[This article is copyrighted as indicated in the article. Reuse of AIP content is subject to the terms at: http://scitation.aip.org/termsconditions. Downloaded to] IP: 147.8.204.164 On: Fri, 19 Sep 2014 07:33:12

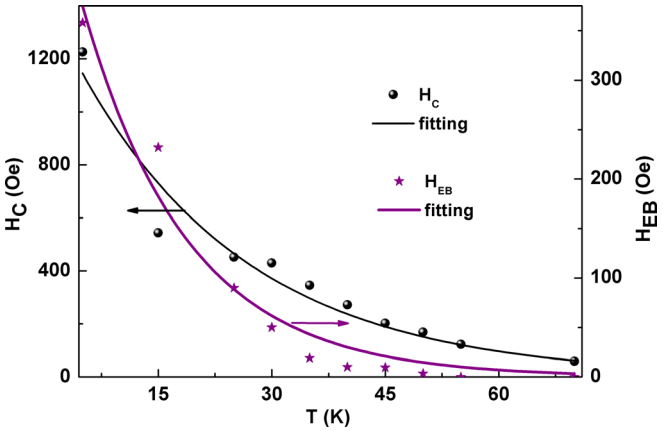

FIG. 4. Temperature dependence of H_{EB} and H_C after 500 Oe field cooling process for L24.

bias (EB) effect in LCMO ultrathin film at low temperatures. In contrast, in the case of strain relaxed L42 sample the EB effect disappears. Representative magnetic loop of L24 at 5 K is shown in Fig. 3(b). The exchange bias field H_{EB} and coercive filed H_C are defined[11] as $H_{EB}=(|H_1|-|H_2|)/2$ and $H_C=(|H_1|+|H_2|)/2$, where H_1 and H_2 are the left and right coercive filed, respectively. The variation of H_{EB} and H_C as a function of film thickness is summarized in Fig. 3(c). What is worth noting is that both values of H_{EB} and H_C are superior to that have been reported in exchange-biased LCMO-based FM-AFM superlattice[12] or nanosystem.[13] It is clear that an effective FM and AFM thicknesses are indispensible for causing strong exchange coupling to induce EB effect. For L3 sample, the magnetic state could be dominated mostly by the AF phase. Hence, the weak coupling between AF and FM cluster gives rise to small H_{EB}. When the film thickness increases, the coupling between FM and AFM phases is energetically modulated. Here, the maximum exchange bias field of 350 Oe and coercive field of 1160 Oe are obtained in L24 sample under 500 Oe cooling field, as shown in Fig. 3(c). Our exchange bias field is also larger than that in many commonly studied system, such as single phase crystal structure $BiFeO_3$ film ($H_{EB}=235$ Oe, $H_c=1130$ Oe)[14] and layered NiFe/FeMn ($H_{EB}=93$ Oe, $H_c=89$ Oe).[15] The absence of bias effect in L42 supports the importance of compressive strain in enhancing the strong phase separation. Further, the effect of training is highlighted in the inset of Fig. 3(c), which describes the decrease of exchange bias field when cycling the system through several consecutive hysteresis loops. The representative relationship between H_{EB} and n for L12 can be well fitted by a simple power law $H_E-H_{E\infty}\propto 1/\sqrt{n}$, where $H_{E\infty}$ is the exchange bias field in the limit of infinite loops.[16] The solid line in Fig. 3(c) shows good agreement with the experimental observations for $n>1$. Such a training effect is commonplace in conventional exchange bias system described within the framework of spin configuration relaxation model.

An exponential temperature-dependent decay of H_{EB} and H_C is unusually observed in glassy system with magnetic frustration.[17] The characteristic dependence of exchange bias field and coercive filed on temperature for L24 is shown in Fig. 4. The data are representative of other samples. Indeed, the temperature dependence of H_{EB} and H_C can be well fitted by the phenomenological formula $H_{EB}(T)=H_{EB}^0\exp(-T/T_1)$, $H_C(T)=H_C^0\exp(-T/T_2)$ where H_{EB}^0 and H_C^0 are the extrapolations of H_{EB} and H_C to the absolute zero temperature; T_1 and T_2 are constants. The fitting results give further resort to scenario that EB effect in LCMO dead layer can be related to the cluster-glass-like state. The blocking temperature T_B of about 50 K, at which H_{EB} diminishes to zero is in good consistent with the corresponding cluster/spin glass-like freezing temperature T_f. The above results suggest that the emergence of cluster/spin glass-like state plays a vital role in EB effect. The coexistence of the FM clusters and AFM clusters will lead to the natural FM/AFM interfaces. Therefore, the origin of EB effect is the exchange coupling between FM and AFM to minimize the interface exchange energy. Moreover, for a cluster, the spins of the shell layer are disordered compared to the core FM ones. The spin disordered shell layer can also act as AFM on the cone FM cluster, which in turn causes the EB effect. Interestingly, the phase separation scenario was also found to be the cause for compressive strained 15 nm thick $La_{0.67}Sr_{0.33}MnO_3$ (LSMO) dead layer previously.[4] Unlike LSMO, the Jahn-Teller distortion and inhomogeneity are more significant in our LCMO magnetic dead layer. Therefore, the bias field and coercive field are found to be promoted by three times under the same cooling field.

III. CONCLUSIONS

In summary, the compressively strained LCMO film exhibits a noticeably contracted unit cell volume compared with that of strain-relaxed, which is ascribed to a stain-enhanced phase separation. The presence of exchange bias effect further demonstrates the coexistence of different magnetic phases in the dead layer. The obtained exchange bias field and the blocking temperature are superior to that have been reported in LCMO-based superlattice or nanosystem.

ACKNOWLEDGMENTS

We acknowledge support from CPSF (No. 2011M500888), NNSFC (Nos. U1332205 and 11274153), NKPBRC (No. 2010CB923404), and NSFHEIJP (No. 11KJB140001).

[1]X. S. Wu *et al.*, J. Appl. Phys. **95**, 7109 (2004).
[2]M. Fu *et al.*, J. Cryst. Growth **312**, 1617 (2010).
[3]S. Liang *et al.*, Appl. Phys. Lett. **95**, 182509 (2009).
[4]Y. H. Sun *et al.*, Phys. Rev. B **78**, 024412 (2008).
[5]Y. L. Qin *et al.*, Philos. Mag. **85**, 4465 (2005).
[6]A. Tebano *et al.*, Phys. Rev. Lett. **100**, 137401 (2008).
[7]Yu. A. Boikov *et al.*, J. Appl. Phys. **96**, 435 (2004).
[8]S. Estradé *et al.*, Appl. Phys. Lett. **91**, 252503 (2007).
[9]M. Bibes *et al.*, Phys. Rev. B **66**, 134416 (2002).
[10]Z. Fang *et al.*, Phys. Rev. Lett. **84**, 3169 (2000).
[11]J. C. Rojas Sánchez *et al.*, Phys. Rev. B **85**, 094427 (2012).
[12]G. Campillo *et al.*, J. Appl. Phys. **99**, 08C106 (2006).
[13]M. H. Zhu *et al.*, Phys. Rev. B **75**, 134424 (2007).
[14]K. D. Sung *et al.*, J. Appl. Phys. **112**, 033915 (2012).
[15]Z. Shi *et al.*, Appl. Phys. Lett. **98**, 122507 (2011).
[16]R. Ang *et al.*, Appl. Phys. Lett. **92**, 162508 (2008).
[17]X. H. Huang *et al.* Phys. Rev. B **78**, 224408 (2008).

[This article is copyrighted as indicated in the article. Reuse of AIP content is subject to the terms at: http://scitation.aip.org/termsconditions. Downloaded to] IP: 147.8.204.164 On: Fri, 19 Sep 2014 07:33:12